NAIC-ID(RS)T-0320-96

NATIONAL AIR INTELLIGENCE CENTER

ANALYSIS OF THE EFFECT OF LIQUID FILM COOLING ON THE PERFORMANCE OF THE TWO-COMPONENT ATTITUDE CONTROL ENGINE

by

Li Ping and Wang Yinfang

DISCLAIMER NOTICE

THIS DOCUMENT IS BEST QUALITY AVAILABLE. THE COPY FURNISHED TO DTIC CONTAINED A SIGNIFICANT NUMBER OF PAGES WHICH DO NOT REPRODUCE LEGIBLY.

HUMAN TRANSLATION

NAIC-ID(RS)T-0320-96 30 September 1996

MICROFICHE NR:

ANALYSIS OF THE EFFECT OF LIQUID FILM COOLING ON THE PERFORMANCE OF THE TWO-COMPONENT ATTITUDE CONTROL ENGINE

By: Li Ping and Wang Yinfang

English pages: 17

Source: Cama, China Astronautics and Missilery Abstracts, Vol. 3, Nr. 1, 1996; pp. 1-8

Country of origin: China
Translated by: Leo Kanner Associates
F33657-88-D-2188
Requester: NAIC/TASC/Richard A. Peden, Jr.
Approved for public release: distribution unlimited.

GRAPHICS DISCLAIMER

All figures, graphics, tables, equations, etc. merged into this translation were extracted from the best quality copy available.

Analysis of the Effect of Liquid Film Cooling on the Performance of the Two-Component Attitude Control Engine

Li Ping and Wang Yinfang

Abstract: By analyzing the operational characteristics of liquid film/radiation cooling of a two-component attitude control engine based on the swirling suction models of two side-zone flow pipes, the authors of this paper divided the combustion chamber flow field approximately into one central zone and two side zones, and calculated the effect of the liquid film cooling of the liquid film/radiation cooling low-thrust liquid rocket engine on its performance loss. Also discussed are the performance analysis results together with the selection of the engine design parameters for an integrated thermal conductivity model. The method presented in this paper can be regarded as a reference for performance calculation and parameter optimization in the design of similar engines.

Key words: liquid film cooling, radiation cooling, performance calculation, attitude control engine

1. Introduction

Generally, the liquid film/radiation cooling is provided to the body of the attitude control-oriented two-component thrust chamber while its outer wall is still under a high temperature. In this case, a large amount of energy has to be scattered to the environment through radiation, and the local loss of performance thus caused can be directly found through the numerical calculations of the integrated thermoconductive model. For the thrust chamber with liquid film/radiation cooling, the specific impulse loss caused by its internal liquid film cooling is even more critical.

In the design of the thrust chamber with liquid film

cooling, a general concern is that the terminal central flow approaches the optimum mixture ratio while the side zones maintain a rather low mixture ratio, because of performance loss from the incomplete fuel combustion inside the thrust chamber.

The cooling liquid film deposited on the wall of the thrust chamber is assumed to be subject to evaporation due to the convection heat flow and radiation heat flow generated by the high-temperature combustion gas coming from the main flow; the film is assumed to continually mix with the central combustion gas flow, to burn and to form the side zones at relatively low temperatures. Subsequently, the mass flow, mixture ratio and temperature in the side zones gradually change along the axial line of the thrust chamber. In calculating the effect of liquid film cooling on the engine performance, this paper divided the chamber into one central main flow zone and two side zones, in accordance with different mixture ratios, just to make calculation simple.

2. Swirling Suction Model of Side Zone Flow Pipe

With the liquid film cooling of straight flow wall-impinging type, all the engines with inclined axial direction have a very small cooling jet flow diameter compared to the combustion chamber diameter and also, very small spacing among cooling holes. Therefore, results from the flat swirling suction and flat jet flow wall-impinging experiment can be used without considering the jet flow concentration caused by the combustion chamber wall curvature. Based on the experiment with wall-impinging cylindrical jet flow movement on a flat plate, we assumed that, under practical working conditions, the liquid film has the same initial distribution on the wall, and we calculated the effect of liquid film cooling on the performance by dividing the combustion chamber flow field into one central zone and two side zones as shown in Fig. 1. Also we assumed that the initial

cooling medium flow rate of the two side zones B1 and B2 respectively are fractions a, and 1-a, of the total cooling fuel flow rate, divided along the circumference. The total cooling liquid film rate is a fraction f of the total flow rate.

During the evaporation period of the liquid film, the Bartz equation, rectified in response to evaporation, can be introduced by the evaporation model in the thermal conductivity analysis. Starting with the evaporation of the liquid film, the main flow of the central zone is drawn into the side zones to form side zone mixed layers with a low mixture ratio. The final mixture ratio of the side zone is determined by the mixture ratio of the side zones at the throat section, which is calculated by the swirling suction model. While in the down stream of the throat, the individual flow pipes are believed to be unmixed. Also, we suppose that:

(1) The central flow is uniform without considering the effect of the design parameters of the other main spray units, including the momentum synthesized angle. Based on the experiment on the wall-impinging jet flow movement, the atomized portion of the initial cooling jet flow is simply believed to have entered the central main flow with the We number as a criterion;

(2) The flow pipes of the two adjacent side zones along the periphery do not mix in the entire process;

(3) The mixture ratio and thermodynamic properties of the central flow do not change with the mixture during the entire process; and

(4) The swirling suction starts with the evaporation of the cooling medium, and the starting point of the full development period of the suction flow is located at the dry spot of the liquid film on the wall, marked as a characteristic spot.

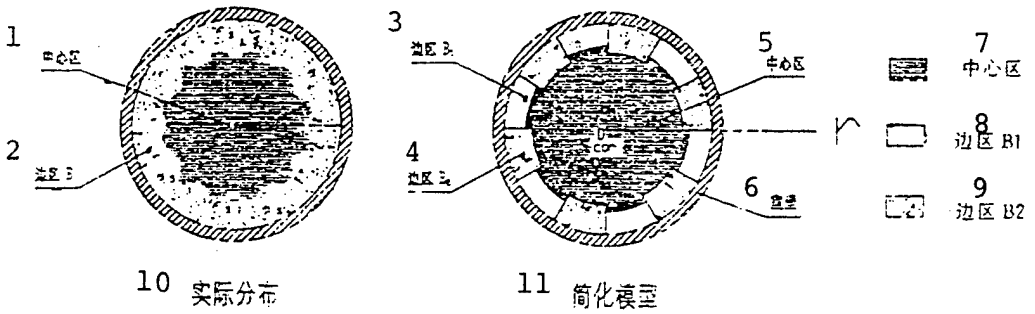

Fig. 1 Simplified Partition in Performance Calculation

Key: (1) Central zone; (2) Side Zone B; (3) Side zone B_1; (4) Side zone B_2; (5) Central zone; (6) Chamber wall; (7) Central zone; (8) Side zone B_1; (9) Side zone B_2; (10) Actual distribution; (11) Simplified model

Under the above assumption, the analysis was made only of the interaction between one side zone flow pipe (presumably flow pipe B_1) and the main flow. Virtually, the side zone is a mixed layer, where the mixture ratio and area in sections along the axial direction of the combustion chamber keep changing, while the mixture ratio of the central flow maintains unchanged along the axial direction.

A suction factor k is defined to represent the speed of the central main flow gas sucked into the side zone flow pipe $\dot{q}_{m.e}$,

$$\dot{q}^{B1}_{m.e}=k\rho_g u_g \qquad (1)$$

where the subscript "g" is the central main flow combustion gas,

the superscript "•" is the unit periphery and the unit length, and the superscript "B1" is the flow pipe B1. The subscript "B1" will be omitted in the following description. Thus, the mass flow rate $q_{m,e}$ of the suction central main flow gas in the mixed layer in an arbitrary axial calculation direction can be derived from Eq. (1). In the swirling suction model, the film cooling efficiency is defined as follows:

$$\eta=(C_g-C_w)/(C_g-1) \tag{2}$$

where the subscript "W" is the near-wall bottom layer, "C" is the cooling medium, and C is the local fuel mass fraction, a conversion value referring to the fuel mass fraction. A full reaction is believed to take place inside the mixed layer in terms of physical properties and other computations, because the chemical reaction is much faster compared to the mixing process. Obviously, the film cooling efficiency defined in the equation is associated with the suction flow rate $q_{m,e}$, cooling medium flow rate $q_{m,c}$ and the mixture ratio shape factor θ in the mixed layer. The mixture ratio shape factor in the mixed layer suggests the degree of mixture development in the mixed layer, which is defined as

$$\theta=\frac{\int_0^{\bullet}\rho u(C_g-C)dr}{(C_g-C_w)\int_0^{\bullet}udr} \tag{3}$$

where S is the thickness of the side zone mixed layer. The cylindrical coordinate r is defined on the inner wall, positively directing at the circular center.

If η is used to give the mixture ratio of the local wall, then

$$MR_w=\frac{1+MRg}{1+\eta MRg}-1 \tag{4}$$

Through the fuel mass conservation in the mixed layer, the following can be derived:

$$q_{m,c}C_c+q_{m,e}C_e=(q_{m,c}+q_{m,e})C_b \tag{5}$$

where the subscript "b" is the overall mean of the mixed layer. By substituting Eqs. (2) and (5) in Eq. (3), the film cooling efficiency, defined based on the suction flow rate $q_{m,e}/q_{m,c}$ and the mixture rate shape factor, η is

$$\eta=\frac{1}{\theta(1+q_{m,e}/q_{m,c})} \tag{6}$$

and the mixture ratio corresponding to the total mass fraction C_b is

$$(MR)_b=\frac{1+(MR)_g}{\theta[\frac{1+MR_g}{1+MR_w}-1]+1}-1 \tag{7}$$

In the initial phase of suction, the mixture has not yet affected the wall layer and at that time, the film cooling efficiency η is 1. Therefore,

$$\theta=(1+q_{m,e}/q_{m,c})^{-1} \tag{8}$$

In the mixture development phase, the efficiency and the shape factor constantly decrease with the increase of $q_{m,e}/q_{m,c}$, but $\eta\to1$, and the mixed layer constantly develops toward the wall. During the full development phase, the mixed layer shape factor no longer changes except for η, which continuously decreases with the increase of suction flow rate $q_{m,e}/q_{m,c}$. The starting point of the full development phase is derived from the characteristic point in the assumption (4).

Based on the experiment of the suction flow of the flat non-acceleration boundary mixed layer as described in Reference [5], the following can be derived:

$$\eta = 1.32/(1+q_{m,e}/q_{m,c}) \tag{9}$$

With reference to Eq. (6), the shape factor in the full development zone is calculated as 0.758. From the initial phase to the start of the full development phase, the shape factor can be approximated by Eq. (8), and the flow rate of the evaporated cooling medium is taken as $q_{m,c}$.

The expression for the suction of the flat non-acceleration flow is

$$q_{m,e}\rho_o u_o S_o = k_o q_{m,c}\rho_g u_g X \tag{10}$$

where S_0 is the thickness of the characteristic point mixed layer; the subscript "0" is the characteristic point in assumption (4).

Based on the experiment of the flat non-acceleration flow of the efficiency as described in Reference [5], the following can be derived:

$$k_o = \frac{0.1}{(\frac{\rho_c}{\rho_g})^{0.15}(\frac{u_c}{u_g})^{0.5}R_{e0}^{0.25}} \tag{11}$$

where R_{e0} takes the thickness of the characteristic point mixed layer S_o as its characteristic dimension. By substituting it in Eq. (10),

$$\eta = [\theta(1+\frac{0.1x}{(\rho_c/\rho_g)^{0.15}(u_c/u_g)^{1.5}R_{e0}^{0.25}})]^{-1} \tag{12}$$

From Eq. (1), in arbitrary location along the axial direction of the combustion chamber,

$$q_{m,e} = \int_0^x 2\pi b(r - S/\cos\alpha)k\rho_g u_g dx \tag{13}$$

where α is the included angle between inner surface of the combustion chamber and the central axial line.

Considering the effect of the main flow acceleration, the suction factor can be given as:

$$k=k_0(\rho_g u_g/(\rho_g u_g)_0)^{\alpha\ \alpha s} \tag{14}$$

In the calculations, the main flow is assumed to accelerate as if there is no side zone liquid film cooling, and the effect of the two-dimensional flow is not counted, then an integral continuous equation is derived as follows:

$$\rho_g u_g=(\rho_g u_g)_0(r_0/r)^2 \tag{15}$$

and the expression of the mixed layer thickness S is

$$(1-\frac{S}{r\cos(\alpha)})^2=(1-\frac{S_0}{r_0})^2(1-\frac{q_{m,g}}{q_m-q_{m,c}}) \tag{16}$$

By substituting Eqs. (14), (15) and (16) in Eq. (13), the integral equation can be solved

$$q_{m,c}=2\pi b(r_0-S_0)k_0(\rho_g u_g)_0\int_0^x(1-\frac{q_{m,c}}{q_m-q_{m,c}})\cdot(\frac{r_0}{r})^{1-2m}k_m(x)dx \tag{17}$$

By connecting $(p_g u_g)$ and S_0 to the flow rate, the following is obtained:

$$\frac{q_{m,c}}{q_m-q_{m,c}}=2\frac{k_0\overline{X}}{r_0-S_0}-[\frac{k_0\overline{X}}{r_0-S_0}]^2 \tag{18}$$

where $$\overline{X}=\int_0^x(\frac{r_0}{r})^{1-2m}k_m dx$$

This way, the convolution flow ratio can be derived and further, other parameters such as film cooling efficiency, side zone mixture ratio can be determined from Eq. (6).

3. Calculation of Liquid Film Cooling Thrust Chamber Performance

The foregoing side zone flow pipe suction model provides a basis for the liquid film cooling performance analysis in the liquid film/radiation cooling thrust chamber. The performance calculation model, rectified in advance with the existing experimental data, can be used, in combination with the suction flow model, to estimate the effect of the liquid film cooling on the performance.

The specific impulse without liquid film cooling I_{sp}, $\Sigma_{,unc}$ can be obtained by subtracting several actual performance losses from the theoretical calculations of the one-dimensional balanced flow under a uniform total mixture ratio of the thrust chamber. Here, the outer radiation heat loss Q_{rad} can be acquired by integrating the theoretical calculations on the thermoconductive model wall temperature along the outer surface of the thrust chamber:

$$dQ_{rad}=q_{rad}(X)dA_s=\epsilon_w\sigma T^4(X)dA_s \tag{19}$$

where ϵ_W is the black body value of the outer wall of the thrust chamber, σ is Stefan-Boltzmann constant, q_{rad} is the radiation heat flow on unit area wall and A_s is lateral area.

According to the second law of thermodynamics, this portion of heat flow cannot be totally converted to kinematic energy. For the convenience of computation, suppose the radiation heat

flow is one-dimensional radial thermal conductivity, then after the pressure of local combustion chamber is given as P, and the jet pipe exit pressure is given as P_e, the local heat flow can be transformed to the kinematic energy efficiency t

$$\eta t = 1 - (P_e/P)^{\frac{k-1}{k}} \tag{20}$$

where k is constant entropy index. Then in the heat flow of the outer radiation loss, the actual part that causes the performance loss is

$$Q' = \int_0^{} 2\pi r \varepsilon \sigma T^4 \eta_k \cos^{-1}\alpha dx \tag{21}$$

In addition, the non-cooling engine specific impulse losses also include reaction kinematic energy losses, boundary layer friction loss, two-dimensional flow loss at the throat and exit, losses caused by the uneven mixture ratio of the central flow, which can define a specific impulse efficiency $\eta t_{sp,\Sigma}$ as follows:

$$\eta_{sp,\Sigma} = \eta_{sp,\ heat}\ \ \eta_{sp,\ others} \tag{22}$$

where $t_{sp,heat}$ can be derived from the above equation, and the last term is various kinds of losses, difficult to calculate, which can be determined based on experience. Thus, $\eta t_{sp,\Sigma}$ is given. At this point,

$$I_{sp,\Sigma,cor} = \eta_{sp,\Sigma} I_{sp,\Sigma,ODE} \tag{23}$$

The specific impulse of the central zone and side zones can also be calculated from the estimation of the total specific impulse of the engine without cooling. Thus, the performance of the engine with cooling can be calculated from the mass weighted mean of the specific impulse of the engine central flow pipe and that of the side zone flow pipes

$$I_{sp,\sum,e} = \eta_{I_{sp},cor} I_{sp,cor,ODE} \frac{q_{m,cor}}{q_m} + \eta_{I_{sp},B1} I_{sp,B1,ODE} \frac{q_{m,B1}}{q_m} + \eta_{I_{sp},B2} I_{sp,B2,ODE} \frac{q_{m,B2}}{q_m} \quad (24)$$

The mass flow rate of the central flow pipe core and the two side zone flow pipes B_1 and B_2--$q_{m,cor}$, $q_{m,B1}$, $q_{m,B2}$, and mixture ratio or excess oxygen coefficient can be determined by the mass flow rate at the throat section, which is calculated by the suction model, while at the down stream of the throat section, no mixture is believed to form, and the mass flow rate of individual flow pipes remains unchanged. As a result, the performance of the thrust chamber and the performance loss caused by liquid film cooling can thereby be derived.

4. Effect of Liquid Film Cooling on Performance and Analysis of Results

The effect of liquid film cooling on the engine specific impulse performance was estimated based on the suction model of the two side zone flow pipes and performance calculations in a model attitude control engine with liquid film/radiation cooling. The initial conditions for the liquid film distribution on the wall was determined according to the liquid flow experiment result. The calculations indicated that under possible practical working conditions and with a smaller liquid film cooling medium fraction f, the mixture ratio exerted a stronger effect on the specific impulse performance loss but the liquid film cooling fraction imposed a relatively minor effect on the specific impulse performance if the cooling was near 10%. Additionally, the highest performance point calculated by using the model was close to the mixture ratio derived from the theoretical calculations of the one-dimensional balanced flow according to an average mixture ratio. When the liquid film cooling fraction rose to a particular point, the effect of the total mixture ratio on the performance was not strong within a wider range, while the

major factor that affected the performance was the liquid film cooling fraction. For instance, near f=22.5%, the performance of the thrust chamber with α=0.65 to α=0.75 is close; near f=22.5%, the performance of the thrust chamber with α=0.70 to α=0.80 is close. To the contrary, when the liquid film cooling fraction continued increasing to a certain degree, the performance of the thrust chamber slightly increased with decrease in the total mixture ratio. The theoretical calculations of the one-dimensional balanced flow of the relative mean mixture ratio approached the optimum mixture ratio point of the thrust chamber, i.e. the higher the overall mixture ratio, the lower the performance of the thrust chamber. Also, based on the thermal conductivity calculations, the higher the overall mixture ratio, the higher the wall temperature of the thrust chamber. In this case, it would be unfavorable for increasing the thrust chamber performance and controlling its wall temperature if the engine was operating under a high mixture ratio. On the contrary, decreasing the mixture ratio would be favorable for both. This suggests that it is undesirable to select a high mixture ratio to increase the performance of similar engines.

Calculations also showed that liquid film cooling could exert a more striking effect on the specific impulse performance of engines working under a rather higher mixture ratio. Meanwhile, with the increase of the fuel liquid film cooling fraction, the decrease of the specific impulse performance due to the change of the liquid film cooling fraction would proceed at a higher rate, which would be even greater if the mixture ratio went higher. If the excess oxygen coefficient α=0.70, the overall specific impulse loss would not exceed 2.7% when the fraction f of the fuel liquid film cooling liquid varied between 10% and 30% (this was confirmed by the ground performance check). When the liquid film cooling fraction continued to increase from 30% to 40%, the performance loss would increase to 3.9%. However, when α=0.65, the corresponding performance loss was

respectively 1.9% and 2.9%.

Figure (2a) shows an engine specific impulse performance estimation curve when α=0.60%-0.80% and liquid film cooling fraction increases from 10% to 40%. Fig. (2b) shows the engine performance estimation curve under different liquid film cooling fractions when α varied between 0.55 and 0.80.

Analysis of data from several thermal test runs of the thrust chamber indicates that the experiment results and model calculations have come to similar conclusions. Fig. (2a) also lists a comparison between calculations and experimental data suggesting that both are in agreement in quantity and change tendency. Nevertheless, there is still a problem with the measurements of the engine operating at low thrust values causing a huge difference among measurement data, which makes it difficult to develop an extensive comparison between theoretical calculations and experimental results.

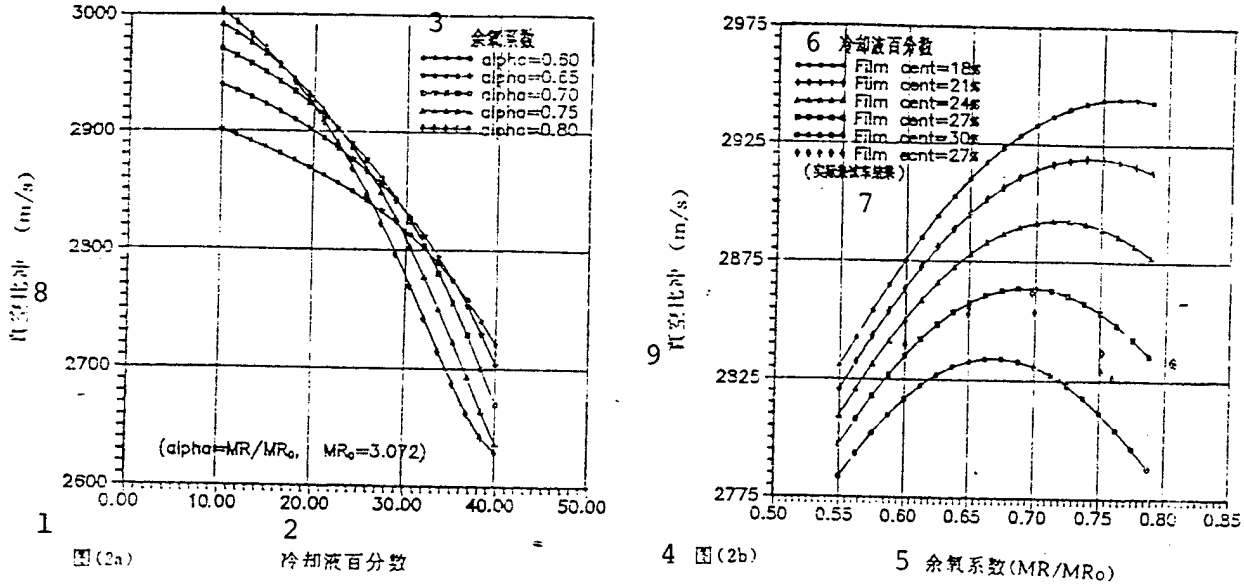

Fig. 2 Effect of Excess Oxygen Coefficient on Performance on Different Liquid Film Cooling Fractions and Effect of Liquid Film Cooling Fraction on Performance Given Different Excess Oxygen Coefficients
(the key to the above figure is given on the following page)

(Key to Figure 2)

Key: (1) Fig (2a); (2) Cooling liquid percentage; (3) Excess oxygen coefficient; (4) Fig (2b); (5) Excess oxygen coefficient (MR/MR_o); (6) Cooling liquid percentage; (7) Actual thermal test run result; (8) Vacuum specific impulse(m/s) ; (9) Vacuum specific impulse(m/s)

Based on the tentative estimation, relatively minor liquid film cooling was adopted in the initial design of that model engine so as to arrive at a higher performance. The thermal test run demonstrated that the performance of the engine conformed to the anticipated value. However, it was found during the experiment that the liquid film cooling was too small while the thrust chamber wall temperature too high. As a result, one of the thrust chambers was burned through at its throat during the experiment.

According to the thermal conductivity analysis made with the performance model for that engine, under the same working conditions the temperature at the throat of the thrust chamber decreases almost linearly with the increase of the cooling liquid film fraction, and the temperature at its wall also decreases with the decrease of the mixture ratio. To solve this problem, it was decided to increase the cooling liquid film fraction and at the same time, to decrease the engine rated excess oxygen coefficient. Decreasing the mixture ratio was good for wall temperature control as well as the constant volume design of the system, yet it caused less performance loss. The major factor that causes the thrust chamber performance loss was an increase of the cooling liquid film fraction, during which the overall specific impulse decreases to 24m/s. A tentative analysis of the improved ground experiment indicates that the result is reliable, but a few more test runs are expected for verification. The selection of the liquid film volume was a little conservative in consideration of the lower wall temperature. This decision was

based on the liquid flow experiment, believing that the limitation of the liquid film cooling hole technology might cause an uneven liquid film cooling on the wall and further, its local superheating.

Calculations suggest that the unevenness of the side zone mixture ratio can not only increase the specific impulse loss of the thrust chamber, but also lead to a local high temperature of the wall, decreasing the reliability of the thrust chamber operation and its service life.

During liquid film cooling, the engine specific impulse loss caused by outer radiation is very small compared with that caused by the liquid film cooling, which, in our experiment, was 9.25m/s when α=0.65 and f=31%, i.e. the performance loss caused by radiation cooling was only 0.3%. And it could be even smaller under other working conditions.

The performance calculations made after a correction was made to k_0 by the throat curvature radius introduced from a reference, as well as the thermal conductivity analysis, were both in disagreement with the thermal test run data. For lack of such research and sufficient data, the effect can hardly be considered for the moment. However, the actual thermal test run result shows that the axial curvature of the throat contractor affects engine performance and thermal conductivity conditions.

The development of the low-thrust two-component engine still remains at the beginning stage in China and thereby is expected to be improved. This paper introduces efforts made in the thrust chamber performance analysis for the research on the two-component attitude control engines. The model presented in this paper, together with the liquid film/radiation cooling thermal conductivity model, may be used to make an integration analysis

of the thrust chamber performance and thermal conditions, and optimize the design parameters in the design of similar engines. Also, it can be used for suggestions for improvement in all design phases based on the integration analysis of the performance model and the thermal conductivity model.

Key to Symbols

Symbol name

a Fraction of side zone flow pipe in cooling liquid

As Circumferential lateral area

C Mass fraction of cooling medium fuel

f Fraction of fuel used for liquid film cooling

I_{sp} Specific impulse

k Suction factor

k_0 Suction factor of flat non-acceleration flow

k_m Flowing or turning correction factor

I Axial length of thrust chamber

m Correction in consideration of flow acceleration

MR Mixture ratio

q_m Overall mass flow rate

$q_{m,c}$ Flow rate of cooling medium

$q_{m,e}$ Mass of suction central main flow

Q_{rad} Radiation disseminated heat flow on outer wall

Q' Part where outer radiation can be converted into kinematic energy

r_0 Diameter of thrust chamber

R_e Reynold's number

S Thickness of mixed layer

u Speed of combustion gas

W'e,We Exit exhaust velocity with and without thermal loss

a Included angle between inner surface of wall and axial line

ηt_{sp} Specific impulse efficiency

ηt Kinematic energy conversion efficiency of outer radiation heat flow

ρ Density of combustion gas

σ Stefan-Boltzmann constant

Subscripts and Superscripts

0 Characteristic point

b Overall mean of mixed layer

B_1, B_2 Flow pipes of two side zones

c Cooling medium

cor Central flow pipe

e Suction

g Central combustion gas

ODE One-dimensional balanced flow's

tl Caused by outer wall thermal radiation

unc Without liquid film cooling

W Under the condition of wall

Σ Overall mean

References

1. Li Ping. Selection of Liquid Film Cooling Design Parameters for Low-thrust Two-component Liquid Rocket Engines and Thermal Conductivity Analysis. Research Institute 11, Aerospace Industry Headquarters, MS Degree Thesis, 1995. 4.

2. Li Ping. Liquid Flow Experiment Report. Inside Report of Institute 11.

3. R. Carl Stechman, Joelee Oberstone. FILM COOLING DESIGN CRITERIA FOR SMALL ROCKET ENGINES, AIAA, Paper, No. 68-617.

4. William M. Grisson. LIQUID FILM COOLING IN ROCKET ENGINES Final report for 1987 to 1989 AEDC-TR-91-1.

5. D. C. Rousar and R. C. Ewen. COMBUSTION EFFECT ON FILM COOLING Final Report NASA-CR-135052.

6. Li Ping, Wang Xinfang and Liang Keming. Thermal Management Design and Thermal Conductivity Analysis of Liquid Film/Radiation Cooling 300N Engine. Proceedings of The Seventh Symposium of Astronautics Association, 1995. 5.

7. А. В. Квасников ТЕОНИЯ ЖИД КОСТНИФ РАКЕТНЫФ ТВИГАТЕЛЕИ